Biochimica et Biophysica Acta, 1028 (1990) 183–199
Elsevier

BBAMEM 74995

Structural dynamics of the Ca^{2+}-ATPase of sarcoplasmic reticulum. Temperature profiles of fluorescence polarization and intramolecular energy transfer

Istvan Jona *, Janos Matko ** and Anthony Martonosi

Department of Biochemistry and Molecular Biology, State University of New York Health Science Center at Syracuse, Syracuse, NY (U.S.A.)

(Received 21 February 1990)

Key words: ATPase, Ca^{2+}-; Fluorescence energy transfer; Molecular dynamics; Calcium ion transport: (Sarcoplasmic reticulum)

The temperature dependence of fluorescence polarization and Förster-type resonance energy transfer (FRET) was analyzed in the Ca^{2+}-ATPase of sarcoplasmic reticulum using protein tryptophan and site-specific fluorescence indicators such as 5-[2-((iodoacetyl)amino)ethyl]aminonaphthalene-1-sulfonic acid (IAEDANS), fluorescein 5′-isothiocyanate (FITC), 2′,3′-*O*-(2,4,3-trinitrophenyl)adenosine monophosphate (TNP-AMP) or lanthanides (Pr^{3+}, Nd^{3+}) as probes. The normalized energy transfer efficiency between AEDANS bound at cysteine-670 and -674 and FITC bound at lysine-515 increases with increasing temperature in the range of 10–37°C, indicating the existence of a relatively flexible structure in the region of the ATPase molecule that links the AEDANS to the FITC site. These observations are consistent with the theory of Somogyi, Matko, Papp, Hevessy, Welch and Damjanovich (Biochemistry 23 (1984) 3403–3411) that thermally induced structural fluctuations increase the energy transfer. Structural fluctuations were also evident in the energy transfer between FITC linked to the nucleotide-binding domain and Nd^{3+} bound at the putative Ca^{2+} sites. By contrast the normalized energy transfer efficiency between AEDANS and Pr^{3+} was relatively insensitive to temperature, suggesting that the region between cysteine-670 and the putative Ca^{2+} site monitored by the AEDANS-Pr^{3+} pair is relatively rigid. A combination of the energy transfer data with the structural information derived from analysis of Ca^{2+}-ATPase crystals yields a structural model, in which the location of the AEDANS-, FITC- and Ca^{2+} sites are tentatively identified.

Introduction

The ATP-dependent translocation of Ca^{2+} across the sarcoplasmic reticulum membrane requires cyclic changes in the structure of the Ca^{2+}-ATPase. Based on kinetic [2–7] and fluorescence data [8–11], it is assumed that during the Ca^{2+} transport cycle the enzyme alternates between two major conformations (E_1 and E_2) with distinct reactivities toward substrates and substrate analogs.

Consistent with these observations the Ca^{2+}-ATPase was crystallized in two distinct conformations under conditions that stabilize the E_1 or the E_2 conformation, respectively [12–15].

The molecular basis of the structural change connected with the $E_1 \rightarrow E_2$ transition remains ill-defined. There are no significant differences between the E_1 and E_2 states in the secondary structures of Ca^{2+}-ATPase determined by circular dichroism [16–17], and only slight differences were observed by Fourier transform infrared spectroscopy [18–20]. While deeper immersion of the Ca^{2+}-ATPase into the bilayer was suggested in some phases of Ca^{2+} transport based on X-ray and neutron diffraction studies [21–22], and electron microscopy [23], the overall shape of ATPase molecules in projection maps of the E_1 and E_2V-type crystals remained similar [12,24], and only their pattern of interactions differed significantly.

Permanent addresses: * Central Research Laboratory, University Medical School, Debrecen, Hungary. ** Department of Biophysics, University Medical School, Debrecen, Hungary.

Abbreviations: FRET, Förster-type resonance energy transfer; SR, sarcoplasmic reticulum; IAEDANS, *N*-iodoacetyl-*N*′-(5-sulfo-1-naphthyl)ethylenediamine; AEDANS, IAEDANS covalently attached to protein; FITC, fluorescein 5′-isothiocyanate; TNP-AMP, 2′,3′-*O*-(2,4,3-trinitrophenyl)adenosine 5′-monophosphate; EGTA, [ethylenebis(oxyethylenenitrilo)]tetraacetic acid, RITC-DPPE, the rhodamine isothiocyanate derivative of dipalmitoylphosphatidylethanolamine.

Correspondence: A. Martonosi, Department of Biochemistry and Molecular Biology, State University of New York Health Science Center at Syracuse, Syracuse, NY 13210, U.S.A.

During recent years several critical intramolecular distances have been determined in the Ca^{2+}-ATPase by Förster-type resonance energy transfer. The high-affinity Ca^{2+}-binding sites have been located using lanthanides as Ca^{2+} analogs, in the alkyl chain region of the bilayer [25,26] about 10 Å from the phospholipid headgroups [27], about 47 Å from the FITC binding site on lysine-515 [28] and about 35 Å from the binding site of TNP-AMP [28]. The intersite distance between the two high affinity Ca^{2+}-binding sites was suggested to be of the order of 8–10 Å [28–31].

IAEDANS preferentially reacts with the Ca^{2+}-ATPase at cysteine-670 and -674 [32,33]. The distance between the bound AEDANS and the binding sites for FITC, TNP-AMP and Pr^{3+} were estimated to be 56, 68 and 16–18 Å, respectively [34]. A distance of 34–43 Å was suggested between rhodamine isothiocyanate labeled dipalmitoylphosphatidylethanolamine incorporated in the phospholipid headgroup region and the FITC bound at lysine-515 [27,35]. Cr-ATP [36] and eosin [37] have also been used to label the nucleotide site. A metal-binding site near the nucleotide-binding region was detected [38], that may represent the subsite involved in the binding of Mg^{2+}-ATP. The height of the ATPase molecule above the cytoplasmic surface of the bilayer, derived from analysis of the Ca^{2+}-ATPase membrane crystals is about 60 Å [13–15,39]. These intersite distances are represented schematically in Fig. 1.

The temperature dependence of Förster-type resonance energy transfer (FRET) can be used to probe fluctuations in donor-acceptor distances and/or orientations [40,41]. The basis of the technique can be briefly summarized as follows: heating the protein gives rise to a greater population of excited vibrational modes characterized by larger vibrational amplitudes. Thus even if the equilibrium distance between donor and acceptor remains the same, the shortest distance between the two will decrease. Since FRET depends on the inverse sixth power of the donor-acceptor distance, these small fluctuations will be expressed in large changes in energy transfer efficiency. The normalized energy transfer parameter [40] will be insensitive to temperature in a rigid structure and the sensitivity to temperature increases with the dynamics of the sampled region of the molecule [40,42].

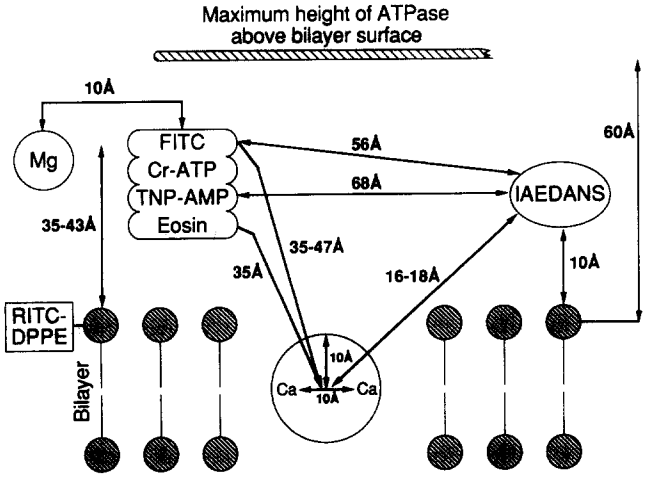

Fig. 1. Intramolecular distances in the Ca^{2+}-ATPase calculated from energy transfer measurements. The indicated distances are compiled from the literature as described in detail in the text. The scheme is not drawn to scale.

The purpose of our studies was to compare the temperature dependence of the distances between the AEDANS, FITC, TNP-AMP and lanthanide-binding sites of the Ca^{2+}-ATPase in the E_1 state stabilized by 0.1 mM Ca^{2+} and in the E_2V state stabilized by 0.1 mM EGTA and 0.5 mM Na_3VO_4. The temperature profiles of FRET and of the polarization of fluorescence of FITC indicate differences in the motional and orientational relationships of covalently bound AEDANS and FITC to each other and to the Ca^{2+}-binding sites noncovalently labeled with lanthanides (Pr^{3+} or Nd^{3+}). A comparison of the temperature dependence of the normalized energy transfer parameter of the different donor-acceptor pairs linked to specific regions of the Ca^{2+}-ATPase in the two principal conformations permitted the tentative identification of 'rigid' and 'soft' regions within the ATPase molecule.

The functional significance of the intramolecular dynamics of Ca^{2+}-ATPase, like that of other proteins and enzymes [43,44], remains to be explored.

A preliminary report was presented at the Annual Meeting of the Biophysical Society on February 21, 1990, in Baltimore, MD, U.S.A., [1].

Materials and Methods

Materials

The sources of materials were as follows. 5-[2-((Iodoacetyl)amino)ethyl]aminonaphthalene-1-sulfonic acid (1,5-I-AEDANS), fluorescein 5′-isothiocyanate (FITC), 2′,3′-*O*-(trinitrophenyl)adenosine 5′-monophosphate (TNP-AMP): Molecular Probes, Eugene, OR, U.S.A. Mops, Tris: Sigma Chemical Co., St. Louis, MO, U.S.A. $PrCl_3$, $NdCl_3$: Alfa Products, Danvers, MA, U.S.A. Na_3VO_4 (ortho): Fisher Scientific Co., Pittsburgh, PA, U.S.A. Ludox light-scattering standard (IBD-1019–69, 30.37% SiO_2, average particle diameter 15.4 nm): gift of E. I. DuPont Nemours and Co. Industrial Chemical Department, Wilmington, DE, U.S.A.

Methods

Preparation of sarcoplasmic reticulum vesicles. SR vesicles were isolated from white skeletal muscles of retired female rabbits according to the procedure of Nakamura et al. [45]. The microsome preparations were stored before use in a medium of 0.01 M Tris-maleate

(pH 7.0), 0.3 M sucrose, at a protein concentration of 24–40 mg/ml, at −70°C. For protein determination the method of Lowry et al. [46] was used. The ATPase activity of the preparations was checked occasionally by a coupled enzyme assay, essentially as described by Varga et al. [47].

Sarcoplasmic reticulum vesicles rather than purified ATPase preparations were used for these studies, because there are strong indications that exposure to detergents irreversibly alters the polarization of tryptophan fluorescence [48] and the infrared spectra of the Ca^{2+}-ATPase [49], accompanied by decrease in the rate of Ca^{2+} accumulation (for review, see [24]). Changes in the distribution of the profile structure of the Ca^{2+}-ATPase with respect to the bilayer [50] were also observed in reconstituted Ca^{2+}-ATPase preparations. These observations suggest that the detergent-treated ATPase preparations currently available may not be suitable for analysis of the finer details of ATPase structure.

Labeling of sarcoplasmic reticulum vesicles with 1,5-IAEDANS and FITC. SR vesicles (5 mg protein/ml) were reacted for 30 min. at 25°C with 1,5-I-AEDANS (4–50 nmol/mg protein) in a medium of 0.1 M KCl, 20 mM Tris-Mops (pH 6.8), 5 mM $MgCl_2$ and 1 mM $CaCl_2$; in some cases the labeling medium was 50 mM Tris-HCl (pH 8.0), 0.3 M sucrose, 0.1 mM EGTA and 5 mM $MgCl_2$. The precise conditions for labeling are given in the Legends. After gel filtration through a Sephadex G-50 column, the microsome fractions were diluted 10-fold with a solution of 0.1 M KCl, 30 mM Tris-Mops buffer (pH 7.0), 5 mM $MgCl_2$ and centrifuged for 50 min at 4°C at $72\,800 \times g$. The sedimented vesicles were resuspended in the appropriate buffer and the protein concentration was determined. The SR vesicles were reacted with FITC according to Papp et al. [51]. In double labeling experiments the reaction with FITC followed the labeling of enzyme with IAEDANS.

The labeling ratios of IAEDANS and FITC were determined from absorbance measurements at 340 nm and 495 nm, respectively, using $\epsilon_{340} = 6.1 \cdot 10^3\ M^{-1} \cdot cm^{-1}$ for IAEDANS [52] and ϵ_{495}: $8 \cdot 10^4\ M^{-1} \cdot cm^{-1}$ for FITC [53]. The absorption measurements were carried out in a Perkin-Elmer Lambda 3B spectrophotometer (Perkin-Elmer Co., Norwalk, CT).

Fluorescence measurements. Most of the fluorescence measurements were carried out in an SLM subnanosecond fluorescence lifetime spectrofluorometer (SLM 4800, SLM Instruments, Urbana, IL, U.S.A.). The temperature was controlled using a circulating waterbath (model RM-6; Lauda Div., Brinkmann Instruments, Westbury, NY). Fluorescence intensities and lifetimes were determined in a ratiometric operation mode, using diluted Ludox suspension as scattering reference. The lifetime of IAEDANS fluorescence was measured at 6 and 18 MHz with the emission monochromator replaced by a Corion (P-10–460-S) interference filter with a bandpass of 10 nm at half height. The lifetimes were obtained and analyzed according to Spencer and Weber [54] and Spencer [55], using the data collection and analysis routine supplied with the instrument.

The intensity and polarization of tryptophan fluorescence of the microsomes was measured at 333 nm using 295 nm light for excitation, with slit widths of 8 and 4 nm for emission and excitation, respectively. The steady-state fluorescence of AEDANS was excited at 340 nm (4 nm slit width) using an XB0 450 W/2 (Osram) xenon arc lamp, and the emission was measured at 480 nm (8 nm slit width). Alternatively, the 365.5 nm line of a 500 W high density mercury lamp (USH-5086A, Japan) was used for excitation of AEDANS fluorescence. The excitation and emission wavelengths of FITC fluorescence were 490 nm and 520 nm, respectively, unless otherwise stated. Polarization of fluorescence was calculated according to Highsmith and Cohen [56].

Fluorescence energy transfer measurements. The efficiency of Förster-type resonance energy transfer (FRET) was determined on SR vesicles labeled with AEDANS or FITC as energy donors and FITC, Pr^{3+}, TNP-AMP or Nd^{3+} as acceptors. The energy transfer $\langle E \rangle$ was calculated from the decrease of donor fluorescence intensity and lifetime in the presence of acceptor. In the determination of $\langle E \rangle$ from steady-state fluorescence intensities the appropriate measured intensities were corrected for inner filter effects by taking into account the optical density increment caused by the additive and for fluorescence emission cross-contribution by subtraction of the fluorescence signal of the fluorophores from the total fluorescence. The average energy transfer efficiency, $\langle E \rangle$, was calculated as:

$$\langle E \rangle = 1 - \langle F_{DA} \rangle / \langle F_D \rangle \text{ or } \langle E \rangle = 1 - \langle \tau_{DA} \rangle / \langle \tau_D \rangle$$

where $\langle F_{DA} \rangle$ and $\langle F_D \rangle$ or $\langle \tau_{DA} \rangle$ and $\langle \tau_D \rangle$ are the population averages of fluorescence intensities and lifetimes of the donor in the presence ($\langle F_{DA} \rangle$, $\langle \tau_{DA} \rangle$) or absence ($\langle F_D \rangle$, $\langle \tau_D \rangle$) of the acceptor. The approximate distances, $\langle r \rangle$, between the donor and acceptor moieties were estimated assuming random orientation using the following equation:

$$\langle r \rangle = R_0 \cdot \left(\frac{1 - E}{E} \right)^{1/6}$$

where R_0 is the critical distance between donor (D) and acceptor (A), when $E = 0.5$, and E is the experimentally determined energy transfer efficiency. For distance calculations $R_0 = 4.9$ nm was used for the AEDANS → FITC pair, and $R_0 = 0.93$ nm for the AEDANS → Pr^{3+} and for the FITC → Nd^{3+} pairs, respectively [34,57].

The temperature dependence of the FRET was analyzed according to the method of Somogyi et al. [40].

The thermal profile of FRET is expected to reflect fluctuations in the donor-acceptor distances as a result of the internal dynamics of the system. The basic conditions required for this kind of analysis [40,42] were tested, and proved to be sufficiently fulfilled in the case of SR-Ca^{2+}-ATPase. One important condition is that the energy transfer depolarization factors (r_D^A) should be relatively independent of the temperature. The emission anisotropy of the acceptor excited through the donor was tested for the AEDANS-FITC pair and showed less than 10% change with temperature in the range of 10–38°C. In the case of the AEDANS-Pr^{3+} and the FITC-Nd^{3+} pairs, χ^2 is close to 2/3 the rapid dynamic isotropic averaging value, and energy transfer depolarization is negligible.

The normalized energy transfer parameter, f, was calculated as $f = \langle E \rangle / \langle \tau_D \rangle$ from time-resolved data, or as $f = \langle E \rangle / \langle F_D \rangle$ from steady-state fluorescence data. The thermal profile of f, $f\langle T \rangle$, is assumed to probe the rigidity/flexibility of the macromolecular environment around or between the fluorophore moieties as described in detail earlier [40,42].

Results

The relationship between the conformation of Ca^{2+}-ATPase and the polarization of tryptophan fluorescence in sarcoplasmic reticulum vesicles

As a preliminary to the studies with extrinsic fluorophores the temperature dependence of the intensity and polarization of the intrinsic tryptophan fluorescence of the Ca^{2+}-ATPase were analyzed.

The intensity of the tryptophan fluorescence of Ca^{2+}-ATPase is larger in the E_1 conformation stabilized by Ca^{2+} or lanthanides, than in the E_2V conformation stabilized by EGTA and vanadate [8,11,58–62]. Membrane potential-dependent changes in the intensity of tryptophan fluorescence have also been observed [11].

The decrease in fluorescence intensity caused by vanadate in the presence of EGTA is accompanied by an increase in polarization at 10°C while there was only slight change at 20°C (Fig. 2A). Mono-, oligo- and decavanadates had similar effects, and the change in polarization approached saturation at millimolar concentrations of vanadate.

By contrast, stabilization of the E_1 conformation by 0.1 mM Ca^{2+} slightly decreased the polarization of tryptophan fluorescence (Fig. 2B); increase in Ca^{2+} concentration from 0.1 mM up to 10 mM had no further effect. The Ca^{2+}-induced decrease in fluorescence polarization was particularly clearly observed when prior to the addition of Ca^{2+}, the endogenous free Ca^{2+} concentration of sarcoplasmic reticulum was reduced by EGTA (Fig. 2C). Alternating additions of EGTA and Ca^{2+} caused alternating changes in fluorescence polarization (Fig. 2C).

The Ca^{2+}-induced decrease in the steady state polarization of tryptophan fluorescence shown in Fig. 2, is in apparent conflict, with a slight increase in the modulated anisotropy of tryptophan fluorescence in the presence of 50 μM Ca^{2+} reported by Gryczynski et al. [63], that was observed at modulation frequencies of 10–100 MHz. The reason for this difference is not clear.

The effect of temperature on the polarization of tryptophan fluorescence

The temperature dependence of the emission anisotropy of tryptophan was analyzed in the E_2V state stabilized by 0.2 mM EGTA and 0.5 mM vanadate, in the E_1 state stabilized by 0.1 mM $CaCl_2$, and in the presence of 0.2 mM EGTA representing a mixture of various subconformations (Fig. 3). The polarization of tryptophan fluorescence decreased with increasing temperature under all three conditions. The temperature profiles of the fluorescence polarization were fully reversible in the range of 10–30°C (not shown), but significant hysteresis occurred after exposure of the vesicles to 37–38°C (Fig. 3). In the range of 10–30°C the change in polarization (ΔP) was slightly greater in the E_2V state (0.012), than in the E_1 state (0.006), or in the presence of EGTA (0.003).

The temperature-dependent changes in tryptophan fluorescence contain contributions from the temperature dependence of all pathways affecting tryptophan orientation and deactivation of the active state [64], including changes in energy transfer depolarization due to temperature-dependent changes in the orientation of and distances between tryptophan residues. The contribution of energy transfer depolarization may be particularly significant [63] in view of the suggested high density of tryptophan residues near the surface of the bilayer [65].

The temperature dependence of the polarization and intensity of the fluorescence of AEDANS and FITC covalently bound to the Ca^{2+}-ATPase

Sarcoplasmic reticulum vesicles were labeled with AEDANS, largely at cysteine-670 and -674 [32,33], or with FITC at lysine-515 [66]; the temperature profiles of fluorescence intensity (Fig. 4) and polarization (Fig. 5) were measured with both types of preparation in the E_1 and E_2V states. The fluorescence intensity of the AEDANS-labeled SR was about 13% higher in the E_1 than in the E_2V state (Fig. 4A) at 10°C, in agreement with [67]. By contrast, the intensity of FITC fluorescence was about 11% higher in the presence of EGTA and vanadate (E_2V), as compared with Ca^{2+}-containing systems (E_1 state) (Fig. 4B), confirming earlier observations [9,10,68]. There was pronounced hysteresis of temperature vs. intensity profiles both with AEDANS and with FITC-labeled SR in the E_1 state after exposure to temperatures higher than 35°C (not shown). Between 10

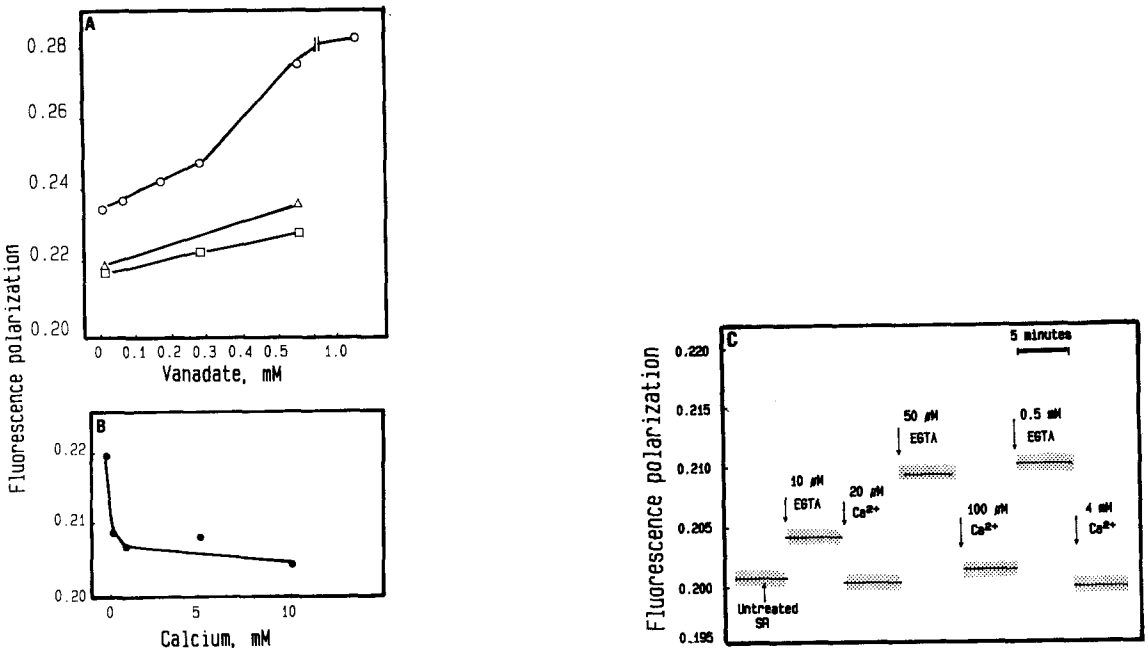

Fig. 2. Effect of vanadate and Ca^{2+} on the polarization of tryptophan fluorescence in sarcoplasmic reticulum vesicles. A. The effect of vanadate. Sarcoplasmic reticulum vesicles (0.1 mg protein/ml) were suspended in 0.1 M KCl, 30 mM Tris-Mops (pH 7.0) and 5 mM $MgCl_2$. The suspension was pretreated with 0.1 mM EGTA, and small aliquots of mono- and decavanadate were added to final concentrations indicated on the abscissa. Symbols: ○, monovanadate, 10°C; □, monovanadate, 20°C; △, decavanadate, 20°C. B. The effect of calcium. To sarcoplasmic reticulum (0.1 mg protein/ml) suspended in 0.1 M KCl, 30 mM Tris-Mops (pH 7.0) and 5 mM $MgCl_2$, small aliquots of $CaCl_2$ were added to final concentrations indicated on the abscissa. Temperature: 20°C. C. Alternating additions of EGTA and Ca^{2+}. To SR vesicles (0.1 mg protein/ml) suspended in the medium described above, aliquots of EGTA and Ca^{2+} were added to final concentrations indicated in the figure. The error (S.E.) of polarization measurements is indicated by the width of the shaded zones.

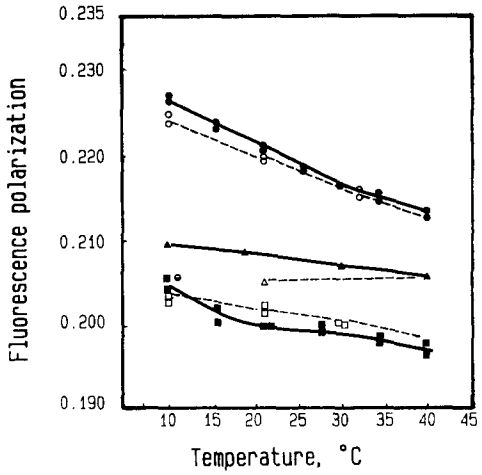

Fig. 3. Temperature dependence of the polarization of tryptophan fluorescence in SR vesicles; the effect of Ca^{2+}, EGTA and vanadate. To SR vesicles suspended in 0.1 M KCl, 30 mM Tris-Mops (pH 7.0), 5 mM $MgCl_2$ (0.15 mg protein/ml), the following ligands were added: 0.2 mM EGTA (△, ▲); 0.2 mM EGTA + 0.5 mM monovanadate (●, ○); or 0.1 mM Ca^{2+} (■, □). After the additions, the samples were warmed in 4–6 steps, each lasting about 5 min, from 10°C to 37°C, and the polarization values were determined at each step (filled symbols). The samples were then cooled stepwise at the same speed to the starting temperature and the polarization was again measured (open symbols). Occasionally duplicates of independent samples were run to determine the error of the measurements. The polarization of SR fluorescence at 10°C without addition of EGTA, Ca^{2+} or vanadate is indicated by ⊖.

and 30°C the intensity of AEDANS fluorescence decreased by approx. 11% both in the E_1 and E_2V states (Fig. 4A); the corresponding changes in the intensity of FITC fluorescence were approx. 15% in the E_1, and approx. 18% in the E_2V state, respectively (Fig. 4B).

The temperature-dependent decrease in the polarization of AEDANS fluorescence was greater than that observed with tryptophan, suggesting greatly increased motional freedom of the covalently bound AEDANS at high temperature, both in the E_1 and E_2V states (Fig. 5).

The polarization of FITC fluorescence remained essentially unaltered by temperature in the E_1 state (Fig. 5A), while in the E_2V state there was a slight increase in polarization at temperatures higher than 25°C (Fig. 5B). The small increase in polarization at high temperature was not completely reversed upon cooling the samples from 37°C to 10°C and may be due to some dissociation of ATPase oligomers together with intramolecular changes.

Energy transfer between AEDANS and FITC covalently bound to the Ca^{2+}-ATPase

Sarcoplasmic reticulum vesicles were labeled with AEDANS at cysteine-670 and -674 and with FITC at lysine-515; the efficiency of energy transfer from AEDANS (donor) to FITC (acceptor) was determined from the effect of acceptor (FITC) on the intensity (Fig.

6) and lifetime (Fig. 7) of donor (AEDANS) fluorescence.

The intensity of AEDANS fluorescence is reduced by FITC at all temperatures in the range of 10–35°C, consistent with energy transfer from AEDANS to FITC. This is accompanied by an increased fluorescence emission by FITC when excited at the excitation maximum of AEDANS (i.e., 365 nm). The energy transfer efficiency calculated from the quenching of donor fluorescence by FITC in the E_1 state stabilized by 0.1 mM Ca^{2+} (Fig. 6A, ●-●) is slightly greater than that in the E_2V state stabilized by 0.1 mM EGTA and 0.5 mM Na_3VO_4 (Fig. 6A, ■-■). Considering the relatively small differences in energy transfer efficiency, one can only conclude that the primary AEDANS sites (cysteine-670 and -674) and the FITC sites (lysine-515) are at similar distances in the E_1 and E_2V states consistent with earlier observations [63,69]. The estimated distances between the two sites, assuming nearly random orientation of the two fluorophores, are 55 ± 1.2 Å in the E_2V and 53 ± 1.3 Å in the E_1 conformation, in reasonable agreement with the observations of Squier et al. [34].

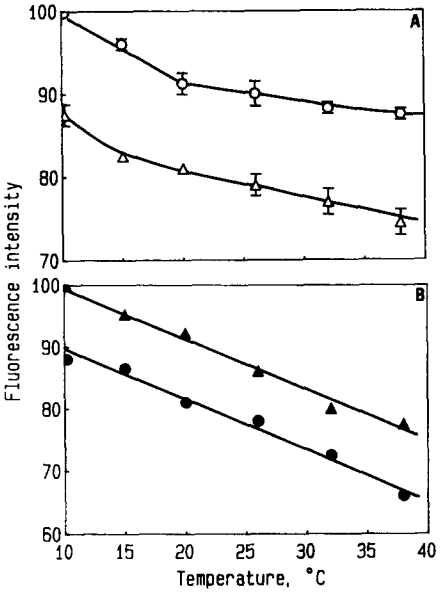

Fig. 4. Effect of temperature, Ca^{2+}, EGTA and vanadate on the fluorescence intensity of 1,5-I-AEDANS and FITC bound to SR vesicles. A. The IAEDANS-labeled SR vesicles (2.9 nmol AEDANS/mg SR protein) were suspended in a medium of 0.1 M KCl, 20 mM K-Mops (pH 7.0), 5 mM $MgCl_2$ (100 μg protein/ml) and 0.1 mM Ca^{2+} (○) was added to stabilize the E_1 state, or 0.1 mM EGTA and 0.5 mM Na_3VO_4 (△) to stabilize the E_2V state. The intensity of the AEDANS fluorescence was measured at 480 nm using an excitation wavelength of 365 nm, at a series of temperatures during stepwise warming from 10 to 38°C, followed by measurements during cooling back to the starting temperature (not shown). Each value represents the average of 200 data points. The AEDANS fluorescence intensities measured in samples containing vanadate were corrected for the absorption increment at 365 nm caused by Na_3VO_4 addition. B. The FITC-labeled SR vesicles (4.9 nmol FITC/mg protein) were suspended in a medium of 0.1 M KCl, 20 mM K-Mops (pH 7.0) and 5 mM $MgCl_2$ to a final concentration of 100 μg protein/ml, and the following additions were made: 0.1 mM Ca^{2+} (●, E_1 state); 0.1 mM EGTA and 0.5 mM Na_3VO_4 (▲, E_2V state). The intensity of FITC fluorescence excited at 490 nm was measured at 520 nm, during warming and cooling, as described above.

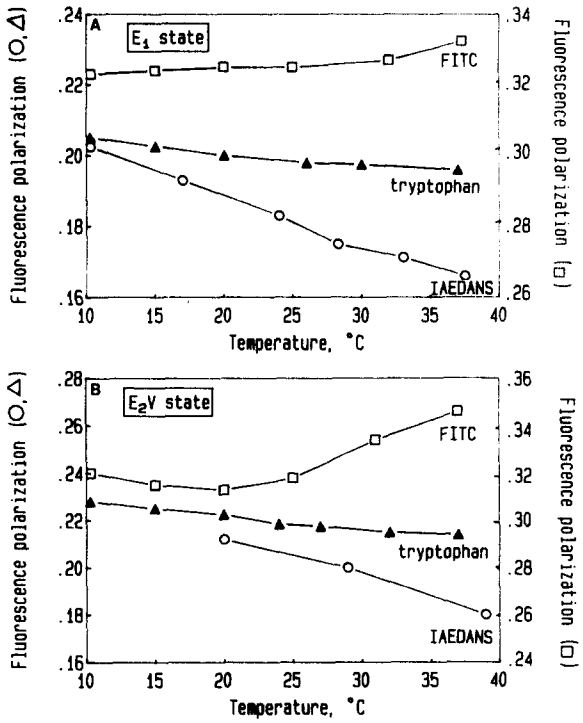

Fig. 5. Temperature dependence of the polarization of FITC, AEDANS and tryptophan fluorescence in sarcoplasmic reticulum Ca^{2+}-ATPase. The effect of Ca^{2+} and vanadate. A. Temperature effects on the polarization of fluorescence in the E_1 state. The unlabeled (▲), FITC-labeled (4.6 nmol FITC/mg SR, □) and AEDANS-labeled (30 nmol AEDANS/mg SR, ○) SR vesicles were suspended in a solution of 0.1 M KCl, 30 mM Tris-Mops (pH 7.0), 5 mM $MgCl_2$, and 0.1 mM $CaCl_2$. Protein concentration: 100 μg protein/ml for unlabeled and 60 μg protein/ml for labeled SR. The polarization of fluorescence of tryptophan (λ_{ex}: 295 nm; λ_{em}: 333 nm, ▲), AEDANS (λ_{ex}: 340 nm; λ_{em}: 480 nm, ○) and FITC (λ_{ex}: 490; λ_{em}: 525 nm, □) were measured at the indicated temperatures as described in Methods. B. Temperature effects on fluorescence polarization in the E_2V state. The unlabeled (100 μg protein/ml) and labeled (60 μg protein/ml) SR vesicles were suspended in 0.1 M KCl, 30 mM Tris-Mops (pH 7.0), 5 mM $MgCl_2$, 0.1 mM EGTA and 0.5 mM Na_3VO_4 and the polarization of fluorescence was determined as described under 'A'.

The temperature-dependent increase in normalized energy transfer (f') calculated from steady state measurements of donor fluorescence (Fig. 6B) was similar in the E_1 and E_2V states at temperatures between 2 and 15°C. At higher temperatures (20–38°C) the normalized energy transfer showed greater temperature sensitivity in the E_2V than in the E_1 state. Since much of the experimental variation shown in Fig. 6A is associated with the measurement of donor fluorescence intensity, after normalization of energy transfer for donor fluorescence these variations are reduced (Fig. 6B). These observations imply slightly greater flexibility of the

AEDANS-FITC region of the Ca^{2+}-ATPase in the E_2V state stabilized by EGTA and vanadate, than in the E_1 state stabilized by Ca^{2+}. This difference arises between 15 and 20°C, where the Ca^{2+}-ATPase is known to undergo a structural transition, as indicated by kinetic and spectroscopic data [2]. Temperature-dependent changes in the profile structure of SR membranes were also seen by X-ray diffraction [22,70].

The energy transfer data based on steady-state fluorescence were supplemented in a limited series of experiments by lifetime measurements of AEDANS fluorescence in the E_1 state at different temperatures (Fig. 7). The principal lifetime of AEDANS fluorescence determined by the phase-modulation technique in the E_1 state in the absence of FITC decreased with increasing temperature from 15 ns at 10°C to 13.1 ns at 30°C (Fig. 7A); in the presence of FITC as energy acceptor the lifetimes were reduced to 12.6 ns at 10°C, and to approx. 10.5 ns at 30°C, indicating significant energy transfer between the AEDANS-FITC pair. The energy transfer $\langle E \rangle = 1 - \langle \tau_{DA} \rangle / \langle \tau_D \rangle$ ranged between 0.18 and 0.24.

Earlier time resolved fluorescence measurements on sarcoplasmic reticulum vesicles labeled with IAEDANS yielded two populations of lifetimes of 18.6–18.8 ns and

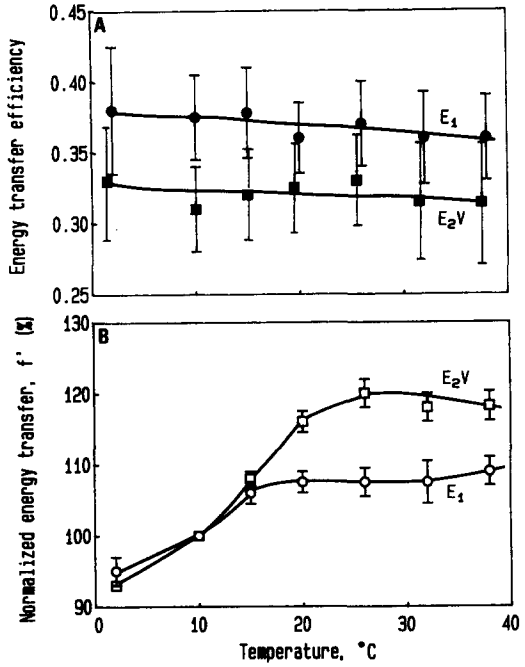

Fig. 6. Temperature dependence of AEDANS-FITC energy transfer and normalized energy transfer in sarcoplasmic reticulum vesicles. Fluorescence intensities were measured at 480 nm using 365 nm light for excitation of AEDANS-SR (donor) or of (AEDANS+FITC) SR (donor+acceptor) systems. For intensity measurements SR vesicles labeled with AEDANS (2.9 nmol AEDANS/mg SR) or with AEDANS (2.9 nmol AEDANS/mg SR) and FITC (4.9 nmol FITC/mg SR) were suspended in 100 mM KCl, 20 mM K-Mops, 5 mM $MgCl_2$ (pH 7.0), containing either 0.1 mM $CaCl_2$ to stabilize the E_1 state (circles) or 0.1 mM EGTA+0.5 mM Na_3VO_4 to stabilize the E_2V state (squares). Protein concentration: 100 μg SR/ml. A. Temperature dependence of the efficiency of FRET. The efficiency of AEDANS-FITC energy transfer, $\langle E \rangle$, was calculated from the steady-state fluorescence intensities of the donor (AEDANS) measured in the absence and presence of acceptor (FITC), as described in Methods. Symbols: ●, energy transfer efficiency in the presence of 0.1 mM Ca^{2+} (E_1 state); ■, energy transfer efficiency in the presence of 0.1 mM EGTA and 0.5 mM Na_3VO_4 (E_2V state); each point represents average of six independent determinations of $\langle E \rangle$ or f'. Error bar corresponds to the standard deviation of these. B. Temperature dependence of normalized energy transfer, f', was calculated from the average energy transfer efficiencies, $\langle E \rangle$, shown in 'A', as described in Materials and Methods. The f' value for data measured at 10°C was taken as 100%. Symbols: ○: normalized FRET in the presence of 100 mM KCl, 20 mM K-Mops, 5 mM $MgCl_2$, 0.1 mM $CaCl_2$ (pH 7.0) (E_1); □, normalized FRET in the presence of 100 mM KCl, 20 mM K-Mops, 5 mM $MgCl_2$, 0.1 mM EGTA, 0.5 mM Na_3VO_4 (pH 7.0) (E_2V).

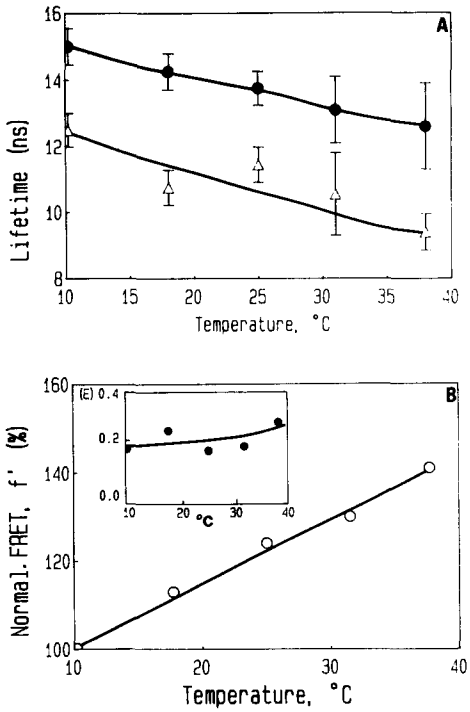

Fig. 7. Effect of temperature on the lifetime of fluorescence of AEDANS in AEDANS-SR and in AEDANS/FITC-SR. A. AEDANS-SR (50 nmol AEDANS/mg SR; 0.25 mg protein/ml, ●) and AEDANS-FITC SR vesicles (50 nmol AEDANS/mg SR; 6 nmole FITC/mg SR, △) were suspended in 0.1 M KCl, 30 mM Tris (pH 7.0), 5 mM $MgCl_2$. The higher labeling ratios with AEDANS were required to minimize noise. The phase and modulation lifetimes were measured at 6 and 18 MHz on SLM 4800 phase fluorometer at the emission and excitation wavelengths described in Methods. The major component of the lifetime obtained from heterogeneity analysis (about 15 ns at 10°C) was close to the apparent lifetime measured at 6 MHz. These values are displayed in the figure with their estimated errors based on the average of 5–8 measurements. B. Temperature dependence of the AEDANS-FITC energy transfer from time-resolved data. The normalized FRET parameter, f', calculated from the $\langle E \rangle$ and $\langle \tau_D \rangle$, as described in Methods, is presented as the function of temperature (○). The energy transfer efficiency, $\langle E \rangle$ (inset), was calculated from the lifetimes of the donor (AEDANS) fluorescence in the absence and presence of acceptor (FITC) as described in Methods (●).

2.5–2.7 ns, respectively [69,71]. According to Birmachu et al. [69], the lifetime of the long lived component was quenched in IAEDANS-FITC labeled preparations to 11.1 ns and 1.2–4.2 ns, respectively, giving two energy transfer distances of 52 Å and 31 Å [69]. We have not observed the component corresponding to the shorter energy transfer distance that may be attributable to nonspecific labeling at sites other than cysteine-670 and -674. Denaturation of the Ca^{2+}-ATPase during the deoxycholate extraction used by Birmachu et al. [69] may have contributed to the nonspecific labeling.

The normalized energy transfer efficiency calculated from the lifetime data ($f = \langle E \rangle / \langle \tau_D \rangle$, %) increased with temperature between 10 and 37°C, consistent with increased motional and/or orientational freedom of donor and/or acceptor fluorophores as the temperature increases (Fig. 7B). The temperature dependence of the effect of FITC on the lifetime of AEDANS fluorescence (Fig. 7) was measured at a higher AEDANS labeling ratio, where sites other than cysteine-670 and -674 may have also become labeled. Nevertheless, the temperature dependence of the AEDANS fluorescence lifetime even under these conditions indicates the same general trend as the energy transfer data based on steady-state fluorescence intensity measurements at low AEDANS labeling ratios (Fig. 6). Further studies are needed to explain whether the difference between the magnitude of the temperature-dependent change in normalized FRET in the E_1 state calculated from lifetime (Fig. 7) and from intensity data (Fig. 6) is fully attributable to the differences in the extent of labeling.

The similar temperature profile of the AEDANS-FITC energy transfer at low and high AEDANS labeling ratios suggests that the heterogeneity of AEDANS distribution, even at the high labeling ratios, is not sufficiently great to exert a major effect on the energy transfer. The Ca^{2+}-ATPase activity of sarcoplasmic reticulum was nearly fully retained even after labeling with 50 nmol of AEDANS per mg protein, in agreement with earlier observations [71].

Energy transfer between AEDANS and praseodymium bound at the cation-binding sites of sarcoplasmic reticulum

Lanthanide ions at submicromolar concentrations interact with the high-affinity Ca^{2+}-binding sites of the Ca^{2+}-ATPase, stabilizing the enzyme in the E_1 conformation [11,12]. At higher lanthanide concentration binding occurs also at secondary cation-binding sites of lower affinity and less-defined specificity [72].

The energy transfer between AEDANS covalently linked to the Ca^{2+}-ATPase as energy donor, and the bound Pr^{3+} as energy acceptor is manifested as quenching of AEDANS fluorescence by Pr^{3+}. The relationship between Pr^{3+} concentration and the efficiency of energy transfer is shown in Fig. 8. The calculated distance between AEDANS at cysteine-670, 674 and the Pr^{3+} bound to the high-affinity Ca^{2+} sites at an ATPase : Pr^{3+} molar ratio of 1 is of the order of approx. 1.8 nm, assuming χ^2 approx. 2/3, in agreement with earlier observations [34]. Significantly smaller distances (approx. 1.3 nm) were obtained at a Pr^{3+} concentration of 9 μM, indicating binding of Pr^{3+} at nonspecific sites.

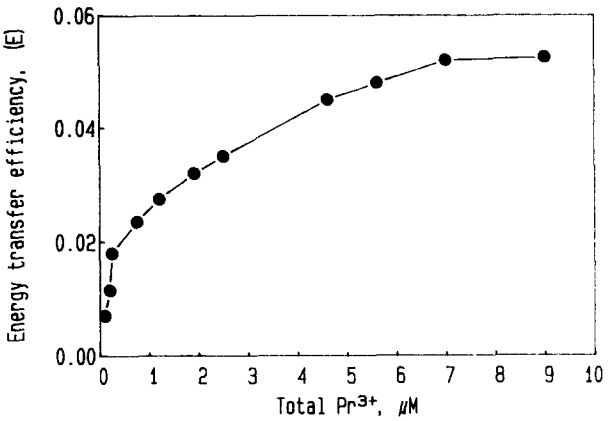

Fig. 8. Energy transfer between AEDANS and Pr^{3+}. The AEDANS-SR (34 nmol of AEDANS/mg SR; 60 μg protein/ml) was suspended in 0.1 M KCl, 30 mM Tris-Mops (pH 7.0), 5 mM $MgCl_2$ and small aliquots of $PrCl_3$ were added to final concentrations indicated on the abscissa. The intensity of AEDANS fluorescence was measured at 480 nm using an excitation wavelength of 340 nm, at 20°C. The energy transfer efficiency was calculated from the quenching of steady-state intensity of donor (AEDANS) fluorescence.

The range of dynamic fluctuation of distances between the covalently linked AEDANS and the high-affinity Ca^{2+}-binding site was analyzed by measuring the temperature dependence of the effect of 1 μM and 9 μM Pr^{3+} on the intensity of fluorescence of AEDANS-labeled ATPase (Fig. 9A). The efficiency of energy transfer is greater at 9 μM than at 1 μM Pr^{3+} concentration, but at both Pr^{3+} concentrations it is nearly independent of temperature between 15 and 32°C (Fig. 9B). Taken together with the very slight dependence on temperature of the normalized energy transfer obtained at 1 μM Pr^{3+} (Fig. 10) these observations imply that the region of the ATPase molecule between the AEDANS site and the high-affinity Ca^{2+} sites is essentially rigid and does not show significant thermally induced structural fluctuations. Surprisingly the normalized energy transfer data obtained at 9 μM Pr^{3+} were also relatively insensitive to temperature (not shown), raising the possibility that the nonspecific cation-binding sites are clustered near the high-affinity Ca^{2+} sites in the ATPase molecule.

Energy transfer between FITC attached at lysine-515 and Nd^{3+} bound at the high-affinity Ca^{2+} site of the Ca^{2+}-ATPase

The fluorescence intensity of FITC covalently bound to the Ca^{2+}-ATPase is reduced by Nd^{3+} bound to the cation-binding sites of sarcoplasmic reticulum due to

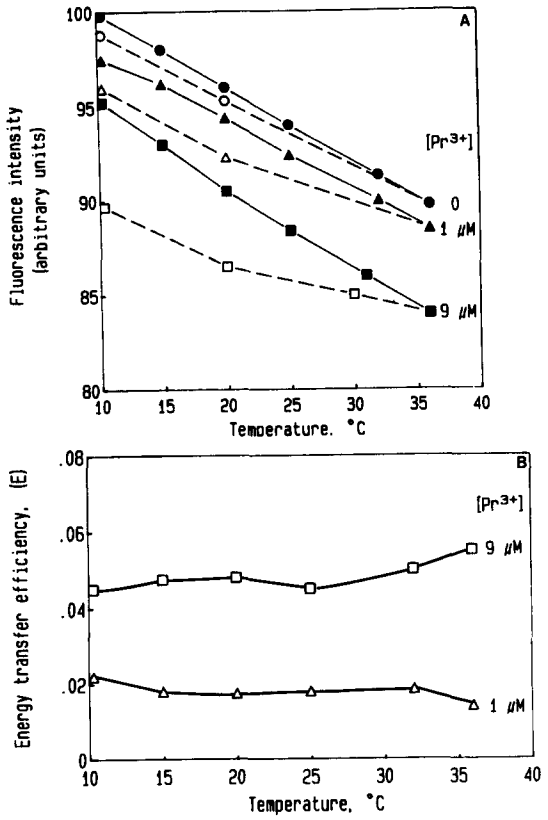

Fig. 9. Temperature effects on the AEDANS-Pr^{3+} energy transfer. A. Temperature dependence of fluorescence intensity of AEDANS-SR was measured in a medium of 0.1 M KCl, 30 mM Tris-Mops (pH 7.0), 5 mM $MgCl_2$ without further addition (●, ○) or in the presence of 1 μM Pr^{3+} (▲, △) or 9 μM Pr^{3+} (■, □) under conditions given in the legend to Fig. 8. The filled symbols refer to intensities measured during stepwise warming and the open symbols to those during cooling of the samples from a starting temperature of 10°C. B. Energy transfer efficiencies in the presence of 1 μM total Pr^{3+} (△), or 9 μM total Pr^{3+} (□) calculated from the data shown under A. Data for the cooling cycle not shown.

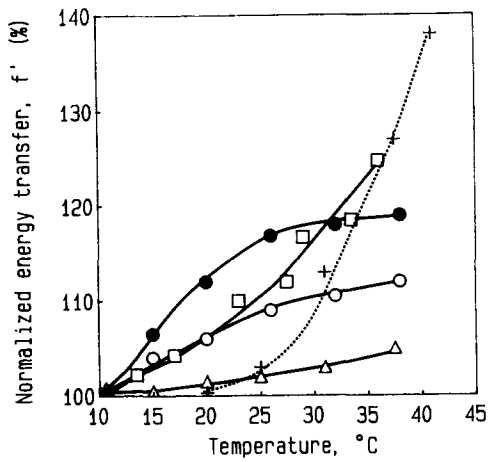

Fig. 10. Temperature dependence of normalized energy transfer, f', for different donor-acceptor systems. The normalized energy transfer, f', was calculated from the average energy transfer efficiencies, $\langle E \rangle$, determined from steady-state intensity data, as described in Methods. The f' value for data measured at 10°C was taken as 100%. For other details see Figs. 6, 9, and 12. Symbols: ○, energy transfer from AEDANS to FITC in the E_1 state (medium: 0.1 M KCl, 30 mM Tris-Mops (pH 7.0), 5 mM $MgCl_2$ + 0.1 mM $CaCl_2$); ●, energy transfer from AEDANS to FITC in the E_2V state (medium: 0.1 M KCl, 30 mM Tris-Mops (pH 7.0), 5 mM $MgCl_2$ + 0.1 mM EGTA, 0.5 mM Na_3VO_4); □, energy transfer from FITC to Nd^{3+} (1 μM); △, energy transfer from AEDANS to Pr^{3+} (1 μM); +, data published by Somogyi et al. [40] on the soluble enzyme RNAse T_1, using tryptophan as donor and pyridoxamine-phosphate as acceptor. In this experiment the f' value determined at 20°C was taken as 100%.

energy transfer. The energy transfer efficiency increases with increase in Nd^{3+} concentration in a biphasic manner; saturation of the high-affinity sites is approached at approx. 3 μM total Nd^{3+} concentration and that of the low-affinity sites at approx. 17 μM Nd^{3+} concentration (Fig. 11). Alternatively there may be negative cooperativity between the Nd^{3+}-binding sites.

The temperature dependence of the energy transfer between FITC as donor and Nd^{3+} as acceptor was analyzed at 1 μM total Nd^{3+} concentration that is assumed to label selectively the high-affinity Ca^{2+}-binding site of the Ca^{2+}-ATPase (Fig. 12). The temperature-dependent change in FITC fluorescence intensity was reversible in the range of 10–30°C, but showed striking hysteresis after exposure to 38°C; this is in accordance with the observations in Fig. 4B that indicated greater sensitivity of the FITC labeled enzyme to temperature-induced structural change in the E_1 state.

The energy transfer between FITC and Nd^{3+} is relatively weak, $\langle E \rangle = 0.011$–$0.018$ (Fig. 12, inset); this is consistent with a minimum distance of approx. 2.2 nm between the two sites. Similar estimates were made earlier by Highsmith and Murphy [57]. The normalized

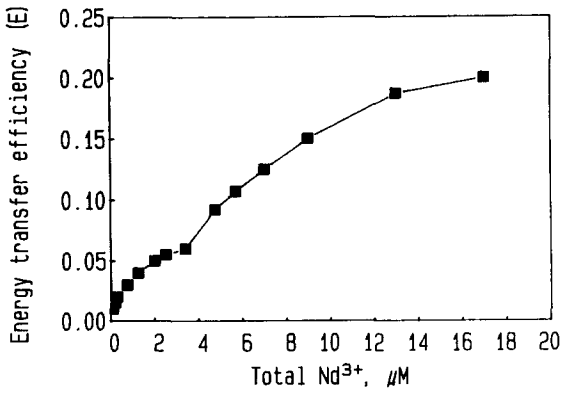

Fig. 11. Energy transfer from FITC to Nd^{3+}. The energy transfer efficiency calculated from the quenching of steady-state fluorescence of donor (FITC) by the bound acceptor (Nd^{3+}) is shown as a function of total Nd^{3+} concentration. The FITC-labeled SR (6 nmol FITC/mg SR, 50 μg protein/ml) was suspended in 0.1 M KCl, 30 mM Tris-Mops (pH 7.0), 5 mM $MgCl_2$ and aliquots of $NdCl_3$ were added to final concentrations indicated on the abscissa. The intensity of FITC fluorescence was measured at 520 nm using an excitation wavelength of 490 nm (slit widths: 4 nm for both sides). Temperature: 20°C.

FRET, or f', increased by about 25% with temperature between 10 and 38°C (Fig. 10), suggesting a temperature-dependent increase in the motional and/or orientational freedom of one or both probes.

The sensitivity of the FITC-Nd^{3+} energy transfer to temperature (Fig. 10) indicates that the region of the Ca^{2+}-ATPase molecule between the high-affinity Ca^{2+} site and the nucleotide-binding domain, that is expected to undergo structural changes during ATP-energized Ca^{2+} translocation, is subject to considerable structural fluctuations, while the region between the Pr^{3+} and the AEDANS sites is relatively rigid (Fig. 10). This is consistent with the independent flexible motion of the domains of Ca^{2+}-ATPase involved in the binding of AEDANS and *N*-(1-anilinonaphth-4-yl) maleimide, respectively [73].

Energy transfer between AEDANS covalently attached to Ca^{2+}-ATPase and TNP-AMP

The fluorescence intensity of IAEDANS covalently bound to the Ca^{2+}-ATPase is reduced by TNP-AMP bound to the substrate binding site due to energy transfer. The energy transfer efficiency increases with increase in TNP-AMP concentration and reaches its half-maximum value at about 0.5–0.6 μM concentration (Fig. 13). The efficiency of energy transfer at 20°C is greater in media containing Ca^{2+} (E_1 state), than in the presence of EGTA and vanadate (E_2V state).

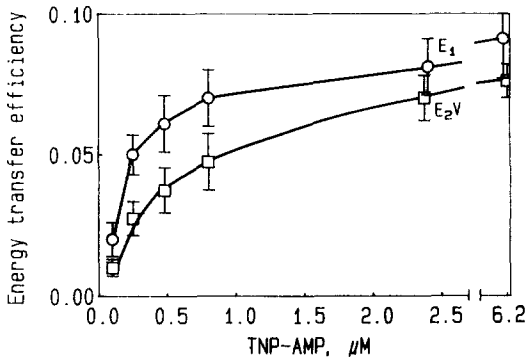

Fig. 13. Effect of TNP-AMP concentration on the efficiency of energy transfer between AEDANS and TNP-AMP. Microsomes were labeled with 2.9 nmol AEDANS/mg SR protein, as described under Materials and Methods. Energy transfer efficiency was determined at 20°C after successive additions of TNP-AMP to final concentrations indicated on the abscissa, followed by measurement of fluorescence emission at 480 nm, using light of 360 nm wavelength for excitation (slit width, 4 nm). Protein concentration: 100 μg AEDANS-SR/ml. Data represent seven independent series of measurements with standard error of the mean, indicated by error bars. Circles: energy transfer efficiency in a medium of 100 mM KCl, 20 mM K^+-Mops, 5 mM $MgCl_2$, 0.1 mM $CaCl_2$ (pH 7.0) (E_1 state). Squares: energy transfer efficiency in a medium of 100 mM KCl, 20 mM K^+-Mops, 5 mM $MgCl_2$, 0.1 mM EGTA, 0.5 mM Na_3VO_4 (pH 7.0) (E_2V state).

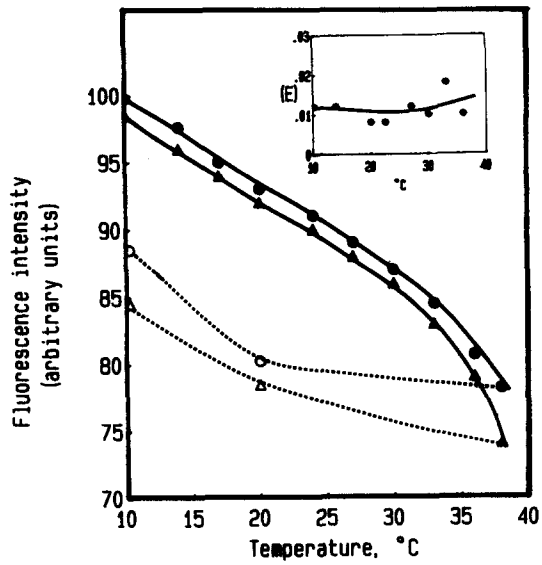

Fig. 12. Effect of temperature on FITC-Nd^{3+} energy transfer. The temperature dependence of the intensity of FITC fluorescence in SR vesicles (6 nmol FITC/mg protein) was measured in the absence (●, ○) or presence (▲, △) of 1 μM total Nd^{3+}, during stepwise warming (●, ▲) and subsequent cooling (○, △) of the samples from a starting temperature of 10°C. The data are averages of 12 measurements of fluorescence intensity at each temperature, with standard deviations ranging from 0.11 to 0.22% of the mean. In view of the small error, the error limits are not indicated for the individual measurements. The corresponding energy transfer efficiencies $\langle E \rangle$ are shown in the inset.

The temperature dependence of energy transfer between AEDANS as energy donor and TNP-AMP as energy acceptor was analyzed at 2 μM TNP-AMP concentration, that nearly saturates the nucleotide-binding site of the Ca^{2+}-ATPase. The temperature dependence of the fluorescence intensity of the donor in the presence of 2 μM acceptor is fully reversible in the E_1 state between 2 and 26°C (Fig. 14B), but in the E_2V state there was significant hysteresis (Fig. 14C).

The normalized energy transfer efficiency (f') decreases with increasing temperature, both in the E_1 and E_2V states (Fig. 14A). The TNP-AMP and FITC are presumed to be attached to similar regions of the ATPase molecule. As the normalized energy transfer efficiency of the IAEDANS-FITC pair increased with temperature both in the E_1 and E_2V states (Figs. 6, 7, 10), the opposite temperature dependence observed with the AEDANS-TNP-AMP pair is surprising and suggests the contribution of some other mechanisms. Since the TNP-AMP is noncovalently attached to the Ca^{2+}-ATPase, we first assumed that the affinity of the TNP-AMP-binding decreases with increasing temperature and the decrease in the energy transfer efficiency may reflect the progressive desaturation of the TNP-AMP-binding site at higher temperatures. The experiments described in Fig. 13 were repeated at 10 μM and at 20 μM TNP-AMP concentrations (not shown), with similar results. Therefore, in addition to slight temperature-dependent change in the affinity of TNP-AMP, a change

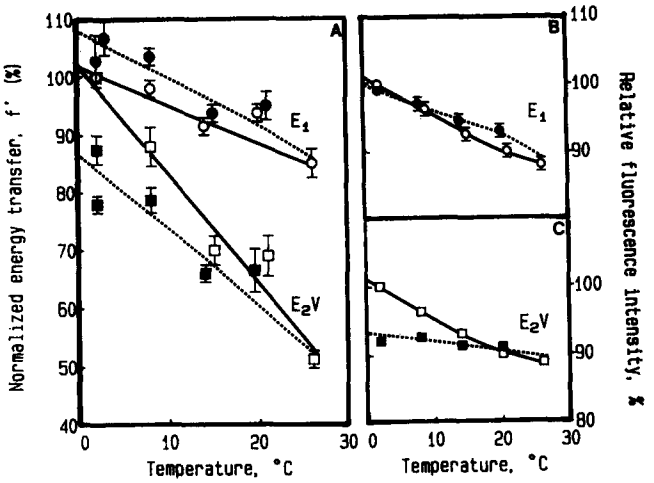

Fig. 14. Temperature dependence of normalized energy transfer from AEDANS- to TNP-AMP. Microsomes were labeled with 2.9 nmol of AEDANS/mg SR protein, as described under Materials and Methods. Fluorescence was measured in a medium of 100 mM KCl, 5 mM $MgCl_2$, 20 mM K-Mops (pH 7.0), 2 μM TNP-AMP and 0.1 mM $CaCl_2$ to stabilize the E_1 conformation (circles) or 0.1 mM EGTA + 0.5 mM Na_3VO_4 to stabilize the E_2V conformation (squares); protein concentration was 100 μg/ml. Each symbol represents the average of 8 independent determinations, the bars indicating the standard error. A. The normalized energy transfer efficiency expressed as percentage of the energy transfer efficiency at 2°C. B, C. The temperature dependence of IAEDANS fluorescence intensities are given in the absence of TNP-AMP in the E_1 medium (B) and in the E_2V medium (C), respectively. Fluorescence was excited at 365 nm and the emission monitored at 480 nm. Open symbols (solid line): warming; filled symbols (broken line): cooling.

in the relative orientation of the two fluorophores is also expected to contribute to the decrease in normalized energy transfer at higher temperatures. This suggestion is supported by temperature-dependent changes in the polarization of TNP-AMP fluorescence.

The excitation spectrum of TNP-AMP is shown in Fig. 15 in the absence and presence of sarcoplasmic reticulum. The spectrum contains at least two components represented by excitation maxima at 408 nm and at 480 nm, respectively, in agreement with the data of Moczydlowski and Fortes [74]. The polarization of fluorescence steadily increased with increase in excitation wavelength between 420 and 500 nm [74]. In the presence of sarcoplasmic reticulum the fluorescence intensity was enhanced several-fold.

A large increase in the polarization of fluorescence of TNP-AMP was observed in the presence of sarcoplasmic reticulum, with increasing temperature at an excitation wavelength of 405 nm (Fig. 16). The polarization of fluorescence was slightly greater at 0.8 μM than at 2.0 μM TNP-AMP concentration at all temperatures in the range of 2 to 26°C, consistent with a larger amount of unbound TNP-AMP being present at the higher (2 μM) TNP-AMP concentration. At both TNP-AMP concentrations the polarization of fluorescence was greater in the E_2V state of the sarcoplasmic reticulum, stabilized by vanadate, than in the E_1 state, stabilized by Ca^{2+}, and the difference in polarization between the two states became more pronounced with

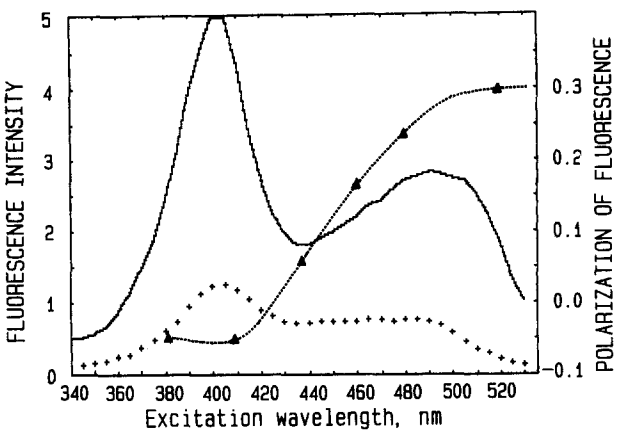

Fig. 15. The excitation spectrum of TNP-AMP and the dependence of fluorescence polarization on excitation wavelength. The fluorescence was measured at 545 nm at the indicated excitation wavelength at 2°C in a medium of 0.1 M KCl, 5 mM $MgCl_2$, 20 mM K-Mops (pH 7.0), at a TNP-AMP concentration of 2 μM without sarcoplasmic reticulum (+) or with 100 μg sarcoplasmic reticulum protein/ml (solid line). The corresponding polarization data (▲···▲) were taken from Moczydlowski and Fortes [74], determined at 0°C at pH 7.5.

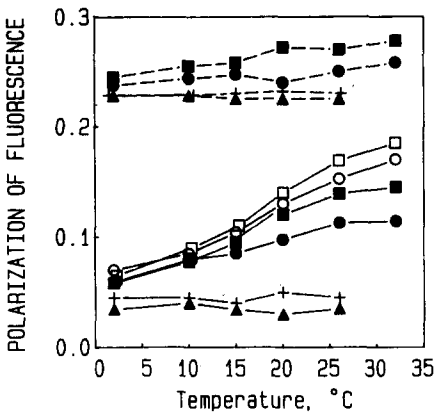

Fig. 16. Temperature profile of the polarization of TNP-AMP fluorescence in sarcoplasmic reticulum vesicles. SR vesicles (100 μg protein/ml) were suspended in a medium of 0.1 M KCl, 5 mM $MgCl_2$, 20 mM K-Mops (pH 7.0) in the presence of 0.8 μM (○, □) or 2.0 μM (●, ■) TNP-AMP, and either 0.1 mM $CaCl_2$ (○, ●) to stabilize the E_1 state, or 0.1 mM EGTA + 0.5 mM Na_3VO_4 (□, ■) to stabilize the E_2V state. The intensity of TNP-AMP fluorescence was measured at 545 nm at a series of temperatures during stepwise warming from 2° to 32°C. The excitation wavelength was either 405 nm (solid lines), or 480 nm (broken lines), corresponding to the two major components of the excitation spectrum shown in Fig. 15. At any given temperature, 200 measurements were averaged. Symbols show the mean of 2 independent sets of measurements; the standard deviations were less than 10% of the mean. The polarization of fluorescence of 2 μM TNP-AMP in the E_1 (▲) and E_2V (+) media, but in the absence of sarcoplasmic reticulum is included as control. The polarization values obtained at 2°C are in close agreement with the polarization data of Moczydlowski and Fortes [74] obtained under similar conditions.

increasing temperature (Fig. 16). Upon return from high to low temperature the polarization of fluorescence decreased with moderate hysteresis (not shown). The intensity and polarization of fluorescence of TNP-AMP in the absence of sarcoplasmic reticulum was low ($P \simeq 0.03$–0.05) when excited at 405 nm and did not change significantly with temperature (Fig. 16).

The polarization of fluorescence measured at an excitation wavelength of 480 nm was much greater at all temperatures compared with the polarization of 405 nm excitation, and changed relatively slightly with temperature, either in the presence or absence of sarcoplasmic reticulum (Fig. 16).

Based on these observations the decrease in normalized energy transfer efficiency with increasing temperature (Fig. 14) is presumably related to the increase in the polarization of TNP-AMP fluorescence seen at 408 nm excitation in the presence of sarcoplasmic reticulum. This change suggests the immobilization of the bound TNP-AMP at high temperature, since the polarization of fluorescence of free TNP-AMP excited at 408 nm remained essentially unchanged between 2 and 26°C.

The effect of pressure on the polarization of TNP-AMP fluorescence

Exposure of sarcoplasmic reticulum to 1.5 kbar pressure for 1 h in the presence of 1 mM EGTA causes nearly complete loss of Ca^{2+}-stimulated ATPase activity [47], accompanied by structural changes in the membrane detectable by FTIR spectroscopy [19,20]. After pressure treatment of sarcoplasmic reticulum at 1.5 kbar for 1 h, the change in the polarization of TNP-AMP fluorescence between 15 and 26°C was sharply reduced (Table I), accompanied by a decrease in ATPase activity from 2.08 to 0.12 $\mu mole \cdot mg^{-1} \cdot min^{-1}$. Vanadate (5 mM) in the presence of 1 mM EGTA protected the enzyme against pressure-induced structural changes [19,20,47]. This protection by vanadate was also expressed in the retention of the fluorescence polarization of TNP-AMP at all temperatures between 2 and 26°C near the level of the control samples maintained at 1 bar pressure; the ATPase activities of the vanadate-containing control (2.56 $\mu mol \cdot mg^{-1} \cdot min^{-1}$) and pressure treated samples (2.41 $\mu mol \cdot mg^{-1} \cdot min^{-1}$) also remained nearly identical. These observations support the conclusion that the polarization of fluorescence of TNP-AMP is dependent upon the native structure of the protein.

Discussion

The thermal profiles of Förster-type energy transfer were explored in the Ca^{2+}-ATPase of sarcoplasmic reticulum using AEDANS-FITC, AEDANS-Pr^{3+}, FITC-Nd^{3+} and AEDANS-TNP-AMP as donor-acceptor pairs. Each of the probes are identified with defined regions of the ATPase molecule. AEDANS is covalently linked to cysteine-670 and -674 [32,33], and FITC to lysine-515 near the nucleotide-binding site [53]. The precise spatial relationship between FITC and the nucleotide-binding domain remains to be determined. Recent observations [75] indicate that ATP at high concentration interacts with the FITC-labeled ATPase, albeit with diminished affinity, indicating that FITC does not block completely the ATP-binding site. The lanthanides are assumed to mark the high affinity Ca^{2+}-sites [26,28,29,76], TNP-AMP, the nucleotide domain and 11 out of 13 tryptophan residues are tentatively located in the membrane spanning regions of the protein near the membrane surface in the headgroup region of phospholipids [65]. Therefore measurement of the distances between these sites in the E_1 and E_2V conformations of the Ca^{2+}-ATPase by FRET provides an experimental test of the proposition [3,16] that the

TABLE I

Temperature dependence of fluorescence polarization of TNP-AMP after pressure treatment

Sarcoplasmic reticulum vesicles (27 mg protein/ml) were pressure treated at 1.5 kbar for 1 h at room temperature in a medium of 0.1 M KCl, 5 mM $MgCl_2$, 20 mM K-Mops (pH 7.0) and 1 mM EGTA or 1 mM EGTA and 5 mM Na_3VO_4. Control samples were kept at atmospheric pressure under the same conditions. Polarization of fluorescence of TNP-AMP (0.8 μM) was measured in a medium of 0.1 M KCl, 5 mM $MgCl_2$, 20 mM K-Mops (pH 7.0) and 0.1 mM EGTA or 0.1 mM EGTA and 0.5 mM Na_3VO_4 at a protein concentration of 100 μg/ml, at the indicated temperatures. For measurements of polarization the samples were warmed up stepwise and the intensity of fluorescence was determined at 545 nm at each temperature using 200 data readings for each setting of the polarizers. The intensities were corrected for blanks (no TNP-AMP) and the value of the polarization calculated. Excitation wavelength was 405 nm with a slit width of 16 nm. Each polarization value is the average (± S.D.) of four or five sets of measurements carried out on two different microsome preparations.

Temperature (°C)	Polarization of fluorescence (P)			
	1 mM EGTA		1 mM EGTA + 5 mM vanadate	
	1 bar	1.5 kbar	1 bar	1.5 kbar
2	0.069 ± 0.002	0.069 ± 0.002	0.060 ± 0.005	0.073 ± 0.015
10	0.080 ± 0.007	0.086 ± 0.007	0.084 ± 0.011	0.083 ± 0.009
15	0.109 ± 0.007	0.105 ± 0.016	0.112 ± 0.016	0.133 ± 0.014
20	0.142 ± 0.013	0.122 ± 0.021	0.150 ± 0.008	0.160 ± 0.023
26	0.166 ± 0.010	0.119 ± 0.008	0.176 ± 0.027	0.176 ± 0.033

conformational change connected with Ca^{2+} transport may involve a relative motion of domains without major rearrangement of the secondary structure of the protein.

The thermal profile of the normalized energy transfer from AEDANS to FITC indicates an about 13% and 20% increase in normalized energy transfer efficiency (f') between 10°C and 38°C, in the E_1 and in the E_2V states, respectively (Fig. 10). Given the nonrandom orientation of donor and acceptor, as indicated by the anisotropy of fluorescence emission, the increase in the normalized energy transfer at higher temperature may reflect increased fluctuation amplitude of the fluorophores, changes in their orientation or average distance, or a combination of these. In any case, the thermal profiles of normalized energy transfer indicate the existence of a relatively soft, flexible structure in the region of the Ca^{2+}-ATPase that links the AEDANS to the FITC site.

The thermal dependence of the normalized transfer efficiency of Ca^{2+}-ATPase, together with earlier observations on the ribonuclease T_1-pyridoxamine 5′-phosphate conjugate [40], and on calmodulin and transferrin [42] support the theory proposed by Somogyi et al. [40] that thermally induced structural fluctuations increase the energy transfer; in fact, the magnitude of the effect in the region of the Ca^{2+}-ATPase sampled by the AEDANS-FITC pair is almost as great as that observed in soluble proteins (Fig. 10).

Considerable thermal fluctuation of structure was also evident in the energy transfer between FITC and Nd^{3+} (Fig. 10); these probes are assumed to sample the regions between the nucleotide binding domain (FITC) and the putative Ca^{2+}-binding domain (Nd^{3+}).

In contrast to these relatively flexible structures, the region monitored by the AEDANS-Pr^{3+} pair appears to be rigid, judged from the insensitivity of the normalized energy transfer efficiency to temperature in the range of 10–37°C (Fig. 9–10). Since specific binding of Pr^{3+} to the high affinity Ca^{2+} sites is plausible only at stoichiometric (1 μM) Pr^{3+} concentration, the similar thermal profile obtained with 1 μM and with 9 μM Pr^{3+} (Fig. 9) may imply that the nonspecific Pr^{3+}-binding also occurs at the cluster of acidic amino acids near the putative Ca^{2+} binding site of the Ca^{2+}-ATPase [65,77,78]. A decrease in the affinity of Pr^{3+} at higher temperature is not likely to account for the absence of the temperature dependence of energy transfer in view of the similar results obtained at 1 μM and 9 μM Pr^{3+} concentration.

It is expected that the temperature dependence of normalized energy transfer would be greater with increasing distances between donor and acceptor fluorophores even if the intervening structures have identical intrinsic flexibility per unit length, because the amplitude of oscillation is likely to increase with length. This trivial explanation cannot satisfactorily account for the observations. The change in normalized energy transfer efficiency with temperature shows no clear relationship with the average distance between donor and acceptor fluorophores either between 10 and 25°C or between 25 and 37°C. Furthermore the normalized energy transfer approaches a plateau above 25°C for the AEDANS-FITC pair, while for the FITC-Nd^{3+} pair it continues to rise up to and above 37°C, and for the AEDANS-Pr^{3+} pair it remains low throughout the whole range of temperatures (Fig. 10).

The binding of TNP-AMP to the Ca^{2+}-ATPase increases the intensity and polarization of TNP-AMP fluorescence in a conformationally sensitive manner, and there is a large further increase in polarization with increasing temperature between 2 and 26°C, both in the E_1 and E_2V states. This implies a reorientation of the probe at higher temperature in an increasingly rigid, hydrophobic environment. Therefore the decrease in normalized energy transfer efficiency between AEDANS and TNP-AMP bound to the Ca^{2+}-ATPase with increasing temperature may be caused by the progressively more unfavorable orientation of the highly immobilized acceptor fluorophore for FET, as the temperature is increased. The unusual temperature dependence of the TNP-AMP fluorescence polarization may also be related to dissociation of ATPase oligomers or to a conformational transition of the native enzyme at elevated temperatures, consistent with earlier observations (for review see [2]). These complications emphasize the caution required in the use of FRET for the analysis of the conformational dynamics of proteins with noncovalently attached probes.

The different behavior of the AEDANS-FITC and the AEDANS-TNP-AMP pairs with respect to the temperature dependence of the normalized energy transfer needs some explanation, in view of the assumed proximity of the FITC and TNP-AMP-binding sites. Although the two sites may be close, they are distinct, and the differences in their behavior probably reflect local differences in the orientational freedom at various temperatures, rather than differences in the structure of the region between the AEDANS and the nucleotide-binding sites of the Ca^{2+}-ATPase. Further studies are needed to assess the contribution of ATPase-ATPase interactions to the polarization of fluorescence of TNP-AMP and to the efficiency of AEDANS-TNP-AMP energy transfer.

Extension of these studies to new donor-acceptor combinations, together with refinement of the structure of Ca^{2+}-ATPase by development of three-dimensional crystals suitable for X-ray diffraction analysis [39,79] may help to identify the structural changes that are involved in Ca^{2+} translocation.

Information about the polarization of fluorescence of donor and acceptor, together with its temperature dependence is a prerequisite for the interpretation of

energy transfer data in terms of distances and fluctuation amplitudes [40,80,81]. The AEDANS-FITC distances calculated assuming random orientation are 5.5 nm in the E_2V conformation stabilized by vanadate and 5.3 nm in the E_1 conformation stabilized by calcium. The assumption of random orientation of the two fluorophores may not be fully justified in view of the high polarization of their fluorescence. The polarization of FITC fluorescence at low labeling ratios is near the limiting polarization (P_0) for fluorescein ([56]; confirmed in this report), and that of AEDANS ($P \cong 0.2$) also indicates a somewhat restricted motion, in agreement with earlier observations of Vanderkooi et al., [71]. The range of distances calculated for orientation factors (χ^2) ranging between 0.33 and 1.3 [82] are 4.9 – 6.1 nm for the E_2V and 4.6 – 5.9 nm for the E_1 state. If the polarization of donor and acceptor are close to 0.3 most of the donor-acceptor pairs have orientation factors in the range $0.33 < \chi^2 < 1.3$ [83,84]. In a recent report, Squier et al., [34] obtained unrealistically low values of polarization for conjugates of Ca^{2+}-ATPase with AEDANS ($P = 0.011$), and FITC ($P = 0.056$); these values were used as a justification for the assumption of random orientation of both fluorophores in energy transfer distance calculations.

The polarization of fluorescence of tryptophan in native sarcoplasmic reticulum ($P \cong 0.2$) is much higher than in most soluble proteins [63,64,85]. The fluorescence polarization of AEDANS, FITC and tryptophan decreased significantly after several days storage of sarcoplasmic reticulum vesicles at 2°C without significant change in ATPase activity. These observations suggest that even relatively subtle changes in the structure of the sarcoplasmic reticulum may alter the conformation of the Ca^{2+}-ATPase, and urge caution in using only fresh preparations for energy transfer measurements.

Solubilization of the Ca^{2+}-ATPase by detergents decreases the tryptophan fluorescence polarization [48], indicating that exchange of membrane lipids by detergents changes the microenvironment of protein tryptophans. This is consistent with spectroscopic evidence allocating the majority of tryptophan residues into a hydrophobic environment [86,87], and with the predicted structure of the Ca^{2+}-ATPase [65] that places 11 out of the total of 13 tryptophan residues in the membrane spanning region, near the headgroups of the phospholipids.

The increase in the intensity of tryptophan fluorescence caused by 0.1 mM Ca^{2+} (E_1 conformation) is accompanied by a decrease in polarization; conversely there is a decrease in tryptophan fluorescence intensity and an increase in polarization in the presence of EGTA and vanadate that stabilize the E_2V conformation. The inverse relationship between the polarization and the intensity of tryptophan fluorescence may arise from quenching interactions of the aromatic side chains, that would be enhanced in the E_2V state shortening the lifetime of excited state and increasing the polarization, while weakened in the E_1 state increasing the lifetime and decreasing polarization. The changes in the second derivative spectrum of the Ca^{2+}-ATPase and the small shift in the emission maximum of tryptophan fluorescence toward shorter wavelengths induced by Ca^{2+} [86] are consistent with such interpretation. A similar mechanism may explain the temperature profile of tryptophan fluorescence polarization that implies increased mobility and/or longer excited state lifetime with increasing temperature; these changes are also more pronounced in the E_2V than in the E_1 state. Other mechanisms that could alter the polarization of tryptophan fluorescence are energy transfer from tyrosine to tryptophan or from tryptophan to tryptophan. We have no explanation for the different effects of Ca^{2+} upon the polarization of tryptophan fluorescence observed by us and by Gryczynski et al. [63], using different techniques on different sarcoplasmic reticulum preparations.

The intensity of AEDANS fluorescence was greater in the E_1 than in the E_2V conformation, while the covalently bound FITC at lysine-515 showed the opposite response, consistent with earlier observations [10,11,67,88]. These changes in the intensity of AEDANS and FITC fluorescence with enzyme conformation were not accompanied by major changes in fluorescence polarization. Therefore the greater efficiency of normalized energy transfer between AEDANS and FITC in the E_2V as compared with the E_1 state at temperatures of 15–38°C (Fig. 10) is likely to indicate changes in the fluctuation amplitude and average distance between the two fluorophores, rather than changes in their relative orientation.

At temperatures between 2 and 15°C there were only slight differences in the AEDANS to FITC energy transfer efficiency between the E_1Ca and E_2V states (Fig. 6), consistent with observations from another laboratory [69]. The Ca^{2+}-ATPase profiles derived from analysis of the E_1 and E_2-type Ca^{2+}-ATPase crystals were also similar [12]. There were only slight differences in FTIR spectra [18,20] and essentially no differences in the circular dichroism spectra [16,17] between the two conformers of the Ca^{2+}-ATPase. Based on these observations Ca^{2+} transport may occur with a structural change that is too small compared with the relatively large error inherent in energy transfer measurements. This is not surprising, since the amplitude of internal motions in proteins rarely exceeds a few Å [89], that would not be detectable with any of the techniques applied so far to the sarcoplasmic reticulum. Therefore no meaningful conclusion can be drawn from the apparent lack of a significant difference in energy transfer efficiency between the E_1 and E_2 states of the Ca^{2+}-ATPase at low temperatures. Interestingly, such dif-

ferences begin to appear in the normalized energy transfer efficiency measured at temperatures closer to the physiological range (approx. 30°C); further exploration of these differences is in progress.

The data presented in this report lead to a revised model of the relationship of the various functional sites of the Ca^{2+}-ATPase to each other and to the membrane bilayer. The most significant change from the original structural model put forward by Brandl et al. [65] is that the Ca^{2+}-binding sites previously located in the stalk helices are now positioned within the bilayer (Fig. 1). In support of this model, mutagenesis of the acidic amino acids in the stalk helices that were originally thought to form the Ca^{2+}-binding domain of the Ca^{2+}-ATPase [65] did not inhibit Ca^{2+} transport [77] while Glu-309, -771 and -908, Asp-800, Asn-796, Thr-799 and Lys-297 of the membrane spanning domains were essential for Ca^{2+} transport [78]. Therefore the transmembrane Ca^{2+} channel is probably formed by a cluster of membrane spanning helices, in analogy to the structure proposed for the Na^{+} channel [90,91] and for other membrane spanning proteins [92]. The observations of Scott [25,26] also indicate effective proximity quenching of the fluorescence of Tb^{3+} bound to the Ca^{2+} sites by doxylstearates in which the nitroxyl group is at positions 12–15, deep in the alkyl chain region of the bilayer. Since Tb^{3+}, like most lanthanides, is expected to stabilize the enzyme in the E_1 state [11,12] and Ca^{2+} translocation occurs in the E_2 state, the Ca^{2+} site is expected to be in the bilayer region in both conformations.

The large apparent distance between the AEDANS and FITC sites places them far apart in the cytoplasmic domain of the Ca^{2+}-ATPase, although they are relatively close in the primary sequence. To match the intramolecular distances derived from energy transfer with the shape of the ATPase molecule determined by reconstruction of Ca^{2+}-ATPase crystals [13–15], we assume that the AEDANS site (cysteine-670 to -674) is located on the lower surface of the lobe [13] portion of the ATPase molecule near the phospholipid headgroups and about $1.6 - 1.8$ nm from the Ca^{2+} site, while the FITC site is on the top of the main cytoplasmic mass forming the bridge, about $3.5 - 4.7$ nm from the Ca^{2+} site. This places the AEDANS and FITC sites at opposite ends of the pear-shaped cytoplasmic domain about 5.0 - 6.0 nm from each other. Such a location of the AEDANS site is supported by studies with monoclonal antibodies directed against the AEDANS binding region of the Ca^{2+}-ATPase [93]. Juxtaposition of the AEDANS and FITC sites located on distinct ATPase molecules within ATPase oligomers may contribute to the energy transfer. Assuming the localization of the AEDANS site on the lower surface of the lobe and of the FITC site on the top of the bridge region of the Ca^{2+}-ATPase [13], the estimated distance between the two sites on adjacent ATPase molecules in the E_2V-type crystals also roughly matches the distance calculated from energy transfer data.

The wide separation between the nucleotide-binding domain and the putative Ca^{2+} transport sites implied by the energy transfer data is frequently taken to indicate long-range energy transfer during Ca^{2+} transport through a propagative change in enzyme conformation [3]. Nevertheless, these observations do not conclusively rule out a more direct effect of enzyme phosphorylation on the gating properties of the Ca^{2+} channel, as suggested by Dupont [94]. More precise data, obtainable only by high-resolution X-ray crystallography will be needed to establish whether the internal motions of the Ca^{2+}-ATPase molecule are sufficient to bring critical elements of the structure within contact distances to effect a direct coupling between the phosphorylation and the Ca^{2+} transport sites.

Acknowledgements

Supported by research grants from the NIH (AR 26545), NSF (PCM 84-03679 and Int. 86-17848) and the Muscular Dystrophy Association.

References

1 Jona, I., Matko, J. and Martonosi, A. (1990) Biophys. J. 57, 500a.
2 Martonosi, A. and Beeler, T.J. (1983) in Handbook of Physiology. Section 10. Skeletal Muscle (Peachey, L.D. and Adrian, R.H., eds.), pp. 417–485, American Physiological Society, Bethesda.
3 Tanford, C. (1984) Crit. Rev. Biochem. 17, 123–151.
4 Inesi, G. and De Meis, L. (1985) in The Enzymes of Biological Membranes, 2nd Edn., Vol. 3 (Martonosi, A., ed.), pp. 157–191, Plenum, New York.
5 Carafoli, E. (1987) Annu. Rev. Biochem. 56, 395–433.
6 Khananshvili, D. and Jencks, W.P. (1988) Biochemistry 27, 2943–2952.
7 Petithory, J.R. and Jencks, W.P. (1988) Biochemistry 27, 5553–5564.
8 Dupont, Y. (1976) Biochem. Biophys. Res. Commun. 71, 544–550.
9 Pick, U. (1982) J. Biol. Chem. 257, 6111–6119.
10 Pick, U. and Karlish, S.J. D. (1982) J. Biol. Chem. 257, 6120–6126.
11 Jona, I. and Martonosi, A. (1986) Biochem. J. 234, 363–371.
12 Dux, L., Taylor, K.A., Ting-Beall, H.P. and Martonosi, A. (1985) J. Biol. Chem. 260, 11730–11743.
13 Taylor, K.A., Dux, L. and Martonosi, A. (1986) J. Mol. Biol. 187, 417–427.
14 Taylor, K.A., Ho, M.-H. and Martonosi, A. (1986) Ann. NY Acad. Sci. 483, 31–43.
15 Taylor, K.A., Dux, L, Varga, S., Ting-Beall, H.P. and Martonosi, A. (1988) Methods Enzymol. 157, 271–289.
16 Csermely, P., Katopis, C., Wallace, B.A. and Martonosi, A. (1987) Biochem. J. 241, 663–669.
17 Nakamoto, R.K. and Inesi, G. (1986) FEBS Lett. 194, 258–262.
18 Arrondo, J.L.R., Mantsch, H.H., Mullner, N., Pikula, S. and Martonosi, A. (1987) J. Biol. Chem. 262, 9037–9043.
19 Buchet, R., Jona, I. and Martonosi, A. (1989) Biochim. Biophys. Acta 983, 167–178.
20 Buchet, R., Carrier, D., Wong, P.T.T., Jona, I. and Martonosi, A. (1990) Biochim. Biophys. Acta 1023, 107–118.

21 Pascolini, D. and Blasie, J. K. (1988) Biophys. J. 54, 669–678.
22 Pascolini, D., Herbette, L.G., Skita, V., Asturias, F., Scarpa, A. and Blasie, J.K. (1988) Biophys. J. 54, 679–688.
23 Peracchia, C., Dux, L. and Martonosi, A. (1984) J. Muscle Res. Cell Motil. 5, 431–442.
24 Martonosi, A., Taylor, K.A., Varga, S. and Ting-Beall, H.P. (1987) in The Electron Microscopy of Proteins, Vol. 6, Membranous Structures (Harris, J.R. and Horne, R.W., eds.), pp. 255–376, Academic Press, New York.
25 Scott, T.L. (1986) Biophys. J. 49, 234a.
26 Scott, T.L. (1988) Mol. Cell. Biochem. 82, 51–54.
27 Teruel, J.A. and Gomez-Fernandez, J.C. (1986) Biochim. Biophys. Acta 863, 178–184.
28 Scott, T.L. (1985) J. Biol. Chem. 260, 14421–14423.
29 Scott, T.L. (1984) J. Biol. Chem. 259, 4035–4037.
30 Herrmann, T.R., Jayaweera, A.R. and Shamoo, A.E. (1986) Biochem istry 25, 5834–5838.
31 Herrmann, T.R. and Shamoo, A.E. (1988) Mol. Cell. Biochem. 82, 55–58.
32 Kawakita, M. and Yamashita, T. (1987) J. Biochem. (Tokyo) 102, 103–109.
33 Bishop, J.E., Squier, T.C., Bigelow, D.J. and Inesi, G. (1988) Biochemistry 27, 5233–5240.
34 Squier, T.C., Bigelow, D.J., de Ancos, J.G. and Inesi, G. (1987) J. Biol. Chem. 262, 4748–4754.
35 Gutierrez-Merino, C., Munkonge, F., Mata, A.M., East, J.M., Levinson, B.L., Napier, R.M. and Lee, A.G. (1987) Biochim. Biophys. Acta 897, 207–216.
36 Herrmann, T.R., Gangola, P. and Shamoo, A.E. (1986) Eur. J. Biochem. 158, 555–560.
37 Kotelnikova, R.A., Tatyanenko, L.V., Mekler, V. M. and Kotelni kova, A.I. (1982) Mol. Biol. 16, 949–954.
38 Highsmith, S. (1984) Biochem. Biophys. Res. Commun. 124, 183–189.
39 Taylor, K.A., Mullner, N., Pikula, S., Dux, L., Peracchia, C., Varga, S. and Martonosi, A. (1988) J. Biol. Chem. 263, 5287–5294.
40 Somogyi, B., Matko, J., Papp, S., Hevessy, J., Welch, G.R. and Damjanovich, S. (1984) Biochemistry 23, 3403–3411.
41 Matko, J., Szollosi, J., Tron, L. and Damjanovich, S. (1988) Q. Rev. Biophys. 21, 479–544.
42 O'Hara, P.B., Gorski, K.M. and Rosen, M.A. (1988) Biophys. J. 53, 1007–1013.
43 Welch, G.R., Somogyi, B. and Damjanovich, S. (1982) Progr. Biophys. Mol. Biol. 39, 109–146.
44 Karplus, M., Brunger, A.T., Elber, R. and Kuriyan, J. (1987) in Cold Spring Harbor Symp. Quant. Biol. LII, pp. 381–390, Cold Spring Harbor Lab, New York.
45 Nakamura, H., Jilka, R.L., Boland, R. and Martonosi, A.N. (1976) J. Biol. Chem. 251, 5414–5423.
46 Lowry, O.H., Rosebrough, N.J., Farr, A.L. and Randall, R.J. (1951) J. Biol. Chem. 193, 265–276.
47 Varga, S., Mullner, N., Pikula, S., Papp, S., Varga, K. and Martonosi, A. (1986) J. Biol. Chem. 261, 13943–13956.
48 Verjovski-Almeida, S., Kurtenbach, E., Amorim, A.F. and Weber, G. (1986) J. Biol. Chem. 261, 9872–9878.
49 Jaworsky, M. and Mendelsohn, R. (1987) Biophys. J. 52, 241–248.
50 Herbette, L., Scarpa, A., Blasie, J.K., Wang, C.T., Hymel, L., Seelig, J. and Fleischer, S. (1983) Biochim. Biophys. Acta 730, 369–378.
51 Papp, S., Pikula, S. and Martonosi, A. (1987) Biophys. J. 51, 205–220.
52 Hudson, E.N. and Weber, G. (1973) Biochemistry 12, 4154–4161.
53 Mitchinson, C., Wilderspin, A.F., Trinnaman, B.J. and Green, N.M. (1982) FEBS Lett. 146, 87–92.
54 Spencer, R.D. (1970) Ph.D. Thesis, University of Illinois at Urbana-Champaign. University Microfilms, Ann Arbor, Michigan.
55 Spencer, R.D. and Weber, G. (1969) Ann. NY Acad. Sci. 158, 361–376.
56 Highsmith, S. and Cohen, J.A. (1987) Biochemistry 26, 154–161.
57 Highsmith, S. and Murphy, A.J. (1984) J. Biol. Chem. 259, 14651–14656.
58 Dupont, Y. (1978) Biochem. Biophys. Res. Commun. 82, 893–900.
59 Dupont, Y. and Leigh, J.B. (1978) Nature London 273, 396–398.
60 Dupont, Y., Bennett, N. and Lacapere, J.-J. (1982) Ann. NY Acad. Sci. 402, 569–572.
61 Guillain, F.P. and Boyer, P.D. (1982) Ann. NY Acad. Sci. 402, 566–568.
62 Guillain, F., Gingold, M.P., Buschlen, S. and Champeil, P. (1980) J. Biol. Chem. 255, 2072–2076.
63 Gryczynski, I., Wiczk, W., Inesi, G., Squier, T. and Lakowicz, J.R. (1989) Biochemistry 28, 3490–3498.
64 Lakowicz, J.R. (1983) Principles of Fluorescence Spectroscopy, Plenum Publ. Co., New York.
65 Brandl, C.J., Green, N.M., Korczak, B. and MacLennan, D.H. (1986) Cell 44, 597–607.
66 MacLennan, D.H., Brandl, C.J., Korczak, B. and Green, N.M. (1985) Nature (London) 316, 696–700.
67 Obara, M., Suzuki, H. and Kanazawa, T. (1988) J. Biol. Chem. 263, 3690–3697.
68 Markus, S., Priel, Z. and Chipman, D.M. (1989) Biochemistry 28, 793–799.
69 Birmachu, W., Nisswandt, F.L. and Thomas, D.D. (1989) Biochem istry 28, 3940–3947.
70 Asturias, F.J. and Blasie, J.K. (1989) Biophys. J. 55, 739–753.
71 Vanderkooi, J.M., Ierokomas, A., Nakamura, H. and Martonosi, A. (1977) Biochemistry 16, 1262–1267.
72 Itoh, N. and Kawakita, M. (1984) J. Biochem. 95, 661–669.
73 Suzuki, S., Kawato, S., Kouyama, T., Kinosita, K., Jr., Ikegami, A. and Kawakita, M. (1989) Biochemistry 28, 7734–7740.
74 Moczydlowski, E.G. and Fortes, P.A.G. (1981) J. Biol. Chem. 256, 2346–2356.
75 Champeil, P., Riollet, S., Orlowski, S., Guillain, F., Seebregts, C.J. and McIntosh, D.B. (1988) J. Biol. Chem. 263, 12288–12294.
76 Highsmith, S.R. and Head, M.R. (1983) J. Biol. Chem. 258, 6858–6862.
77 Clarke, D.M., Maruyama, K., Loo, T.W., Leberer, E., Inesi, G. and MacLennan, D.H. (1989) J. Biol. Chem. 264, 11246–11251.
78 Clarke, D.M., Loo, T.W., Inesi, G. and MacLennan, D.H. (1989) Nature 339, 476–478.
79 Pikula, S., Mullner, N., Dux, L. and Martonosi, A. (1988) J. Biol. Chem. 263, 5277–5286.
80 Haas, E. and Steinberg, I.Z. (1984) Biophys. J. 46, 429–437.
81 Demchenko, A.P. (1986) Essays Biochem. 22, 120–157.
82 Dale, R.E. and Eisinger, J. (1976) Proc. Natl. Acad. Sci. U.S.A. 73, 271–273.
83 Dale, R.E., Eisinger, J. and Blumberg, W.E. (1979) Biophys. J. 26, 161–193.
84 Haas, E., Katchalski-Katzir, E. and Steinberg, I.Z. (1978) Biochemistry 17, 5064–5070.
85 Chen, R.T. and Edelhoch, H. (1975) Biochemical Fluorescence, Marcel Dekker, Inc., New York.
86 Restall, C.J., Coke, M., Phillips, E. and Chapman, D. (1986) Biochim. Biophys. Acta 874, 305–311.
87 Ferreira, S.T. and Verjovski-Almeida, S. (1989) J. Biol. Chem. 264, 15392–15397.
88 Suzuki, H., Obara, M., Kubo, K. and Kanazawa, T. (1989) J. Biol. Chem. 264, 920–927.
89 McCammon, J.A. and Harvey, S.C. (1987) Dynamics of Proteins and Nucleic Acids, Cambridge University Press.

90 Noda, M., Shimizu, S., Tanabe, T., Takai, T., Kayano, T., Ikeda, T., Takahashi, H., Nakayama, H., Kanaoka, Y., Minamino, N., Kangawa, K., Matsuo, H., Raftery, M.A., Hirose, T., Inayama, S., Hayashida, H., Miyata, T. and Numa, S. (1984) Nature 312, 121–127.
91 Noda, M., Ikeda, T., Kayano, T., Suzuki, H., Takeshima, H., Kurasaki, T., Takahashi, H. and Numa, S. (1986) Nature 320, 188–192.
92 Lodish, H.M. (1988) Trends Biochem. Sci. 13, 332–334.
93 Molnar, E., Seidler, N.W., Jona, I. and Martonosi, A. (1990) Biochim. Biophys. Acta 1023, 147–167.
94 Dupont, Y. (1983) FEBS Lett. 161, 14–20.